Materials Horizons

A Photopolymerizable Thermoplastic with Tunable Mechanical Performance

Journal:	*Materials Horizons*
Manuscript ID	MH-COM-08-2019-001336.R1
Article Type:	Communication
Date Submitted by the Author:	09-Nov-2019

Complete List of Authors:	Alim, Marvin; University of Colorado Boulder, Materials Science & Engineering Childress, Kimberly; University of Colorado Boulder, Chemical and Biological Engineering Baugh, Neil; University of Colorado Boulder, Chemical and Biological Engineering Martinez, Alina; University of Colorado Boulder, Materials Science & Engineering Program Davenport, Amelia; Colorado Photopolymer Solutions Fairbanks, Benjamin; University of Colorado Boulder, Chemical and Biological Engineering McBride, Matthew; University of Colorado Boulder, Chemical and Biological Engineering Worrell, Brady; University of Colorado Boulder, Chemical and Biological Engineering Stansbury, Jeffrey; University of Colorado Boulder, Chemical and Biological Engineering McLeod, Robert; University of Colorado Boulder, Electrical, Computer, and Energy Engineering Bowman, Christopher; University of Colorado Boulder, Chemical and Biological Engineering

COMMUNICATION

A photopolymerizable thermoplastic with tunable mechanical performance

Received 00th January 20xx,
Accepted 00th January 20xx

DOI: 10.1039/x0xx00000x

Marvin D. Alim,*[a] Kimberly K. Childress,[b] Neil J. Baugh,[b] Alina M. Martinez,[a] Amelia Davenport,[c] Benjamin D. Fairbanks,[b] Matthew K. McBride,[b] Brady T. Worrell,[b] Jeffrey W. Stansbury,[bd] Robert R. McLeod[ae] and Christopher N. Bowman [abf]

Semicrystalline polymeric materials possessing extraordinary mechanical properties were rapidly fabricated using light from low viscosity liquids at room temperature. Unlike conventional photopolymerizations which form crosslinked networks, this material is a noncrosslinked polymer which renders it meltable and intrinsically reprocessable. This introduces a new class of high performance, recyclable materials applicable for light-based additive manufacturing.

Additive manufacturing (3D printing), widely regarded as the next frontier in prototyping, production and manufacturing,[1-3] is a rapidly evolving technology for the fabrication of highly complex and customized materials.[3] In particular, light-based 3D printing, or stereolithography (SLA), is regarded as the state-of-the-art technique for the production of high quality parts,[4-6] offering a superior combination of cost, throughput, customizability and resolution. Although SLA printing technologies have advanced tremendously in terms of print speed,[6-9] methodology,[8-11] multi-material printing,[12, 13] and achievable resolutions,[7-10, 12] the materials produced, even with post-processing,[14] are predominantly highly crosslinked thermosets because solid parts are manifested by crosslinking almost instantaneously upon irradiation, which supports high pattern resolutions, and uses widely available, low cost monomers. For these reasons, the majority of SLA 3D printing resins are effectively restricted to the radical chain-growth polymerizations of multifunctional (meth)acrylates,[3, 4, 7, 8, 11, 12, 14-18] and/or cationic curing of epoxides.[12, 13, 19] While a diverse and valuable array of material properties has been achieved through extensive formulation engineering (comprising various monomers and oligomers, reactive/unreactive diluents, additives, stabilizers), there are fundamental limitations intrinsic to all chain-growth multi(meth)acrylate systems such as low pre-gel conversions, significant shrinkage stress buildup, and embrittlement. In addition, viscosity constraints for resin reflow further restrict what is constituted as printable.[3, 15] Therefore, achieving an encompassing range of properties for SLA 3D printing with multi(meth)acrylate photopolymers alone is intractable.

To extend the useful but limited material property space of standard (meth)acrylates, multiple researchers have explored various strategies towards the ultimate goal of high performance, functional SLA 3D prints[4, 11, 12, 14-18, 20-22] demonstrating elastomeric-like materials,[14, 15, 20-22] thermoset reprocessability,[11] enhanced toughness,[18, 20] multi-material printing,[12, 13] and even using the thiol-ene or other polymerization reactions as alternate resin curing chemistries.[11, 20, 23-27] However, all these approaches fundamentally involved the fabrication of an insoluble, crosslinked polymer with limited work[16, 17] on the vat photopolymerization of thermoplastic polymers. Thermoplastics, such as poly(ethylene terephthalate) (PET), are the defining synthetic materials of modern society based on their unmatched combination of (re)processability, overall cost, and tunable range of material properties that facilitate countless uses. Despite their undoubted utility, producing thermoplastic materials, or even close mimics, via photopolymerization remains an unresolved challenge. In this regard, important work from Long and coworkers introduced novel strategies to 3D print all-aromatic polyimides comparable to commercial Kapton, although the printing involved high resin viscosities with the final polyimide only achieved via a thermal post-processing step that led to significant shrinkage of the final part.[16, 17] Significantly, while multiple researchers have

[a] Materials Science and Engineering Program, University of Colorado Boulder, Boulder, Colorado 80309, USA.
[b] Department of Chemical and Biological Engineering, University of Colorado Boulder, Boulder, Colorado 80309, USA.
[c] Colorado Photopolymer Solutions, Boulder, Colorado 80301, USA.
[d] Department of Craniofacial Biology, School of Dental Medicine, University of Colorado Denverr, Aurora, Colorado 80045, USA.
[e] Department of Electrical, Computer and Energy Engineering, University of Colorado Boulder, Boulder, Colorado 80309, USA.
[f] Biofrontiers Institute, University of Colorado Boulder, Boulder, Colorado 80309, USA.

† Footnotes relating to the title and/or authors should appear here.
Electronic Supplementary Information (ESI) available: Experimental details and characterization methods. See DOI: 10.1039/x0xx00000x

developed and used various methods to form linear or non-crosslinked polymers via thiol-X reactions,[28-31] none of these approaches result in photopolymer materials of sufficient mechanical integrity to be considered viable thermoplastic materials for most applications, especially additive manufacturing. Therefore, to the best of our knowledge, there has been little, if any, published work on the direct SLA-based 3D printing of truly robust linear polymers. Here, as shown in **Scheme 1**, the defining virtues of both thermoplastics and photopolymers are combined into a single materials platform, extending thermoplastic materials to be photopolymerizable and, more specifically, geared towards additive manufacturing. Utilizing a unique subset of dithiol and divinyl monomers, we demonstrate that semicrystalline high molecular weight polymers are rapidly produced under neat conditions at ambient temperature and low irradiation intensities (1-10 mW cm^{-2}). Owing to the high molecular weights and extent of crystallinity quickly achieved in these photopolymerizable thermoplastic systems, impressively tough materials closely resembling important thermoplastics, such as PET, are formed. Crucially, we validate applicability towards vat photopolymerization-based 3D printing of thermoplastic objects and/or molds for other objects that are subsequently melted and/or reprocessed.

Inspired by the structure of PET, the first interaction with photopolymerizable thermoplastic systems entailed the observation of an initially transparent and colorless film of a linear thiol-ene system, hereon referred to as HDT-DAT and comprising a stoichiometric combination of 1,6-hexane dithiol (HDT) and diallyl terephthalate (DAT) with 2,4,6-trimethylbenzoyl diphenylphosphine oxide (TPO) as the photoinitiator, photopolymerized in bulk that turned white and opaque after several hours. This polymer film was remarkably resistant to mechanical deformation with a storage modulus on the order of 100 MPa in tension (at 20°C) and physically

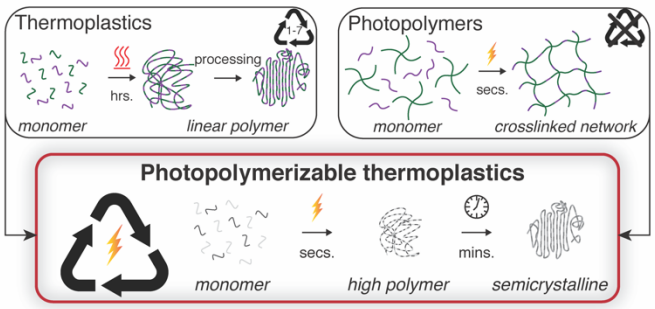

Scheme 1. Overview of the photopolymerizable thermoplastics materials paradigm. Conventional thermoplastics typically involve thermally-driven polymerizations to form high molecular weight polymers that vary in degree of branching and degree of crystallinity. In contrast, photopolymers comprise the light-induced formation of permanently crosslinked networks, which are predominantly amorphous. The presented system, photopolymerizable thermoplastics, harnesses the thiol-ene 'click' reaction to combine the key characteristics of both systems, i.e. the light-induced formation of robust, linear polymers.

resembled classical semicrystalline thermoplastics with elongation to break of up to 800%. Investigations of this material paradigm consisted of a series of in-situ experiments to provide fundamental insight on the various processes occurring in these photopolymerizable thermoplastics with the HDT-DAT system described herein as a representative system. First, rapid reaction kinetics achieving near quantitative conversions of both thiol and ene groups was confirmed using real-time Fourier transform infrared spectroscopy (FTIR) with 405 nm LED irradiation at a low exposure intensity (10 mW cm^{-2}) as shown in Figure 1A. The effectively identical kinetic profiles of both thiol and ene groups suggests a nearly ideal step growth polymerization process with minimal vinyl homopolymerization observed and times to complete conversion that were less than 3-5 seconds despite the low intensity and ambient curing conditions. The rapid polymerization kinetics observed here is essential for SLA 3D printing of a resin to be practical.

COMMUNICATION

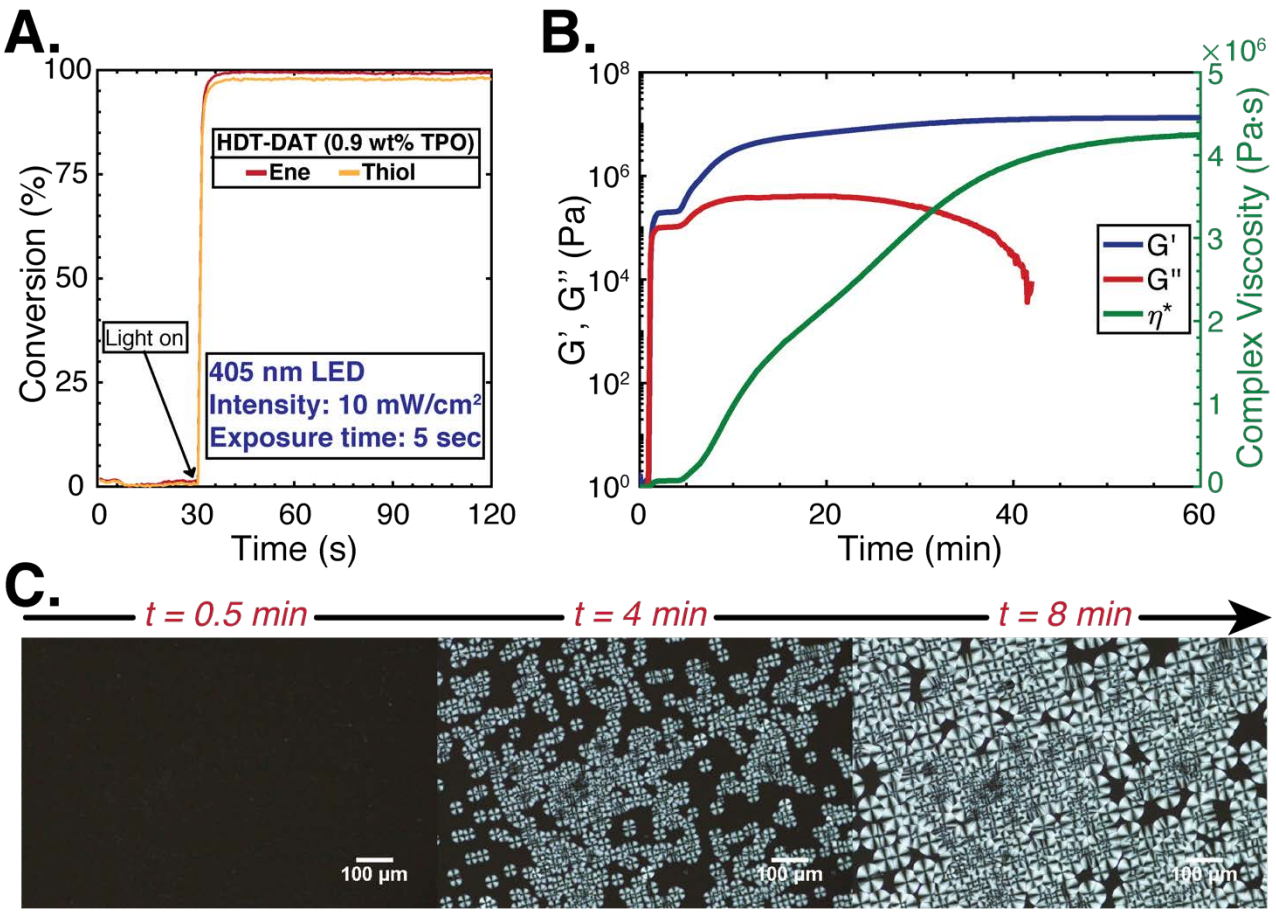

Figure 1. Bulk real-time characterization of the HDT-DAT photopolymerizable thermoplastic system. (a) Reaction kinetics via real-time FTIR of the thiol-ene photopolymerization using a 5 s irradiation (405 nm LED, 10 mW/cm^2) showed nearly-instantaneous, quantitative conversions of both thiol and ene groups. (b) Real-time modulus development obtained via photo-rheology (405 nm LED, 10 mW/cm^2; continuous irradiation from t = 60 s) revealed a sharp increase in both storage (G') and loss (G'') modulus due to the photopolymerization, with an eventual decrease in G'' below the instrumental detection limits. Critically, G' continued to increase well after the polymerization before eventually hitting a plateau due to crystallization. This phenomenon was also revealed in the concomitant increase in the complex viscosity (η*). (c) Representative optical images taken with crossed polarizers of the photopolymerization and subsequent crystallization processes upon a uniform 400 nm LED irradiation. The characteristic Maltese cross patterns gradually appear and grow in size until impingement with each other.

Next, as shown in Figure 1B, the modulus development of the thermoplastic photopolymer system was studied with real-time photo-rheology to measure both storage (G') and loss moduli (G'') upon identical 405 nm irradiation conditions. As expected, the moduli increased dramatically due to the photopolymerization with a rapid G'-G'' crossover (indicative of solid-like behavior) observed with a momentary plateau in moduli. However, unique to this system, it was discovered that G' continues to further increase well after the polymerization had completed and the polymer molecular weight was no longer increasing, before eventually hitting a final plateau. This phenomenon was also revealed in the concurrent and dramatic increase in the complex viscosity (η*) of the system as shown on the secondary y-axis of Figure 1B. Based on this rheological data and the visual observation of changes in physical appearance of the polymer (i.e. going from transparent to translucent to white), it was hypothesized that polymer crystallization was occurring with the preceding modulus plateau attributed to a duration of polymer organization. To directly confirm crystallization, *in-situ* polarized microscopy imaging of the photopolymerization and crystallization processes was conducted with a series of representative time points presented in Figure 1C. This experiment showed the development of characteristic spherulites over several minutes – well after light exposure and the polymerization were complete as determined from real-time FTIR. Curiously, initial

spherulites were observed to grow preferentially at the exposure interface presumably due to favorable heterogenous nucleation potentially associated with intermediate molecular weights and heightened mobility associated with a small amount of residual monomer in this transition zone. After this initial growth, spherulites coalesce inwards until they impinge on each other with the inner centroid developing at a later time. The ability and propensity for crystallization in these particular thiol-ene systems is explained by the quantitative conversions resulting in long polymer chains that possess high degrees of linear symmetry, mimicking the semicrystalline PET structure.[32] Thus, the produced polymers are expected to be minimally branched with significant stereoregularity and a regular step-growth configuration (i.e. marginal homopolymerization). Furthermore, in analogy to PET, crystallization is promoted by the combination of the flexible alkyl chains to aid in self-organization,[32-34] the intermolecular dipole-dipole interactions between the polar carbonyl groups,[35] as well as the regular π-π stacking of the benzene rings present along the main chain. Systems studied employing the 1,2-substituted (diallyl phthalate) and 1,3-substituted (diallyl isophthalate) structural isomers instead of the 1,4-substituted DAT were not observed to be crystalline following polymerization with HDT (Supporting Information Figure S1 and Figure S2). Classically, spherulite formation (crystallization) in polymers has been observed from either melts or solutions involving a large degree of undercooling ($\Delta T = T_m - T_c$, the difference between melting and crystallization temperatures) and slow cooling rates;[36-39] however, as demonstrated here, the crystallization of a polymer formed and subsequently kept at ambient temperature was evidenced within a very short timescale (seconds to minutes, depending on the formulation and conditions, as opposed to hours).

While the presence of crystallinity in the HDT-DAT polymers is generally indicative of linear polymers, the formation of a non-crosslinked polymer is unequivocally confirmed by either its ability to melt, flow, or be dissolved in a suitable solvent. First, as shown in Figure 2A, differential scanning calorimetry (DSC) using standard heat-cool-heat ramp cycles confirmed both a relatively sharp melting endotherm with a peak of 78°C and a broader exothermic transition of crystallization between 7 and 22°C. The presence of an additional, albeit less pronounced, crystallization exotherm (at approximately 55°C to 75°C) was attributed to domains of higher degree of crystallinity. The detection of distinct first-order phase transitions (i.e. melting and crystallization) further supports the notion of semicrystalline linear polymers being produced from these rapid thiol-ene photopolymerizations. While a defined glass transition temperature was not detected via DSC, temperature scans with a dynamic mechanical analyzer (DMA) in tension revealed a tan δ peak occurring around -14°C (Supporting Information Figure 3). Furthermore, solubility tests conducted in a variety of common organic solvents showed full dissolution in both DCM and THF at a concentration of 1 mg/mL (Supporting Information Table S1) ruling out crosslinking that would lead to a gelled structure. Rather unsurprisingly, the insolubility of the

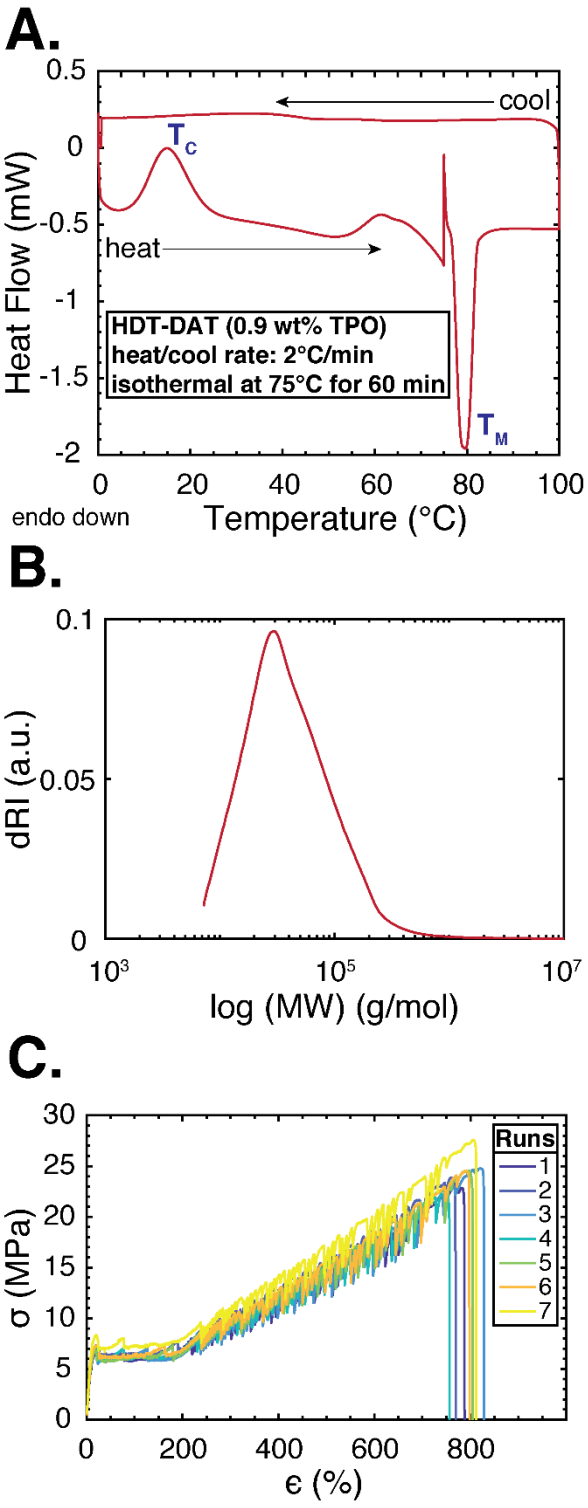

Figure 2. Thermal transitions, molecular weight and mechanical properties of HDT-DAT photopolymerizable thermoplastic system. a) Dynamic scanning calorimetry scans reveal distinct first-order phase transitions – melting and crystallization. b) Size exclusion chromatography with multi-angle light scattering (MALS) eluted in THF confirm linear polymers of $>10^4$ g mol^{-1} (differential refractive index signal is plotted against molecular weight, calculated from MALS). c) Representative uniaxial tensile stress-strain performance of 150 µm thick HDT-DAT ASTM D638 Type V dogbones (bulk photopolymerized films cut into shape using a mold cutter) and tested at a strain rate of 5 mm-min^{-1} at ambient conditions (n=7) revealed extremely tough materials with a unique strain hardening mechanism.

polymers in numerous conventional solvents such as toluene is consistent with the well-known solvent characteristics of PET.

As high molecular weights are the defining characteristic for functionally useful linear polymers[32, 35], absolute molecular weights (MW), dispersity and chain morphology (degree of branching) of HDT-DAT were determined using size-exclusion chromatography with multi-angle light scattering and differential viscometry (SEC-MALS) in tetrahydrofuran (THF). A representative plot for HDT-DAT is shown in Figure 2B, corresponding to number-average molecular weights on the order of 10^4 g mol^{-1}. Based on log-log plots of intrinsic viscosity (η) versus molar mass (M) (i.e. Mark–Houwink–Sakurada plots shown in Supporting Information Figure S4), a random coil morphology was determined with an exponent of 0.46; these results were consistent with the observed tendency towards crystallization. According to the Carothers equation,[40] achieving these molecular weights in a linear step-growth system (corresponding to degree of polymerizations approaching 100) would entail near-perfect stoichiometric balance (r = 1) and conversions of about 99% or greater. Generally speaking, these requirements are unattainable for most polymerization methods, let alone, photopolymerizations. Possible explanations of these high step growth molecular weight results are limited to either: i) a pure thiol-ene step-growth polymerization, ii) a predominantly ideal thiol-ene mechanism with a minor contribution from the homopolymerization of the diallyl ester that leads to branching, or iii) significant ene homopolymerization. The first hypothesis is unlikely because commercial monomers were used as received with relatively large ranges in purity possible which when coupled with typical experimental errors in weighing out the monomers would result in a stoichiometric imbalance between the reactive functionalities that was greater than that necessary to achieve these molecular weights. The third hypothesis was also effectively ruled out by the solubility of the polymer in organic solvent as a diallyl homopolymerization would produce intractable covalently crosslinked networks and would also lead to significantly different conversions of the thiol and ene as measured by FTIR. Therefore, it was deduced that the thiol-ene step-growth was the predominant polymerization mechanism with further increases in molecular weight supported by small amounts of homopolymerization of any residual ene groups to produce linear polymers with low degrees of branching. This premise is supported by recent studies by Liska and coworkers where they investigated the reactivity of vinyl esters (close analogs to the allyl esters used in these studies) with thiols against their (meth)acrylate(s) structural counterparts.[41] This study revealed that thiol-vinyl ester photopolymerizations proceeded significantly faster than the vinyl ester homopolymerization and could even outpace the kinetics of acrylate homopolymerizations. These rapid kinetics were attributed to the differences in resonance stabilizations of the acrylate and vinyl ester radicals leading to different monomer and radical reactivities.[42] Vinyl ester radicals, as opposed to acrylate (α-carbonyl) radicals, lack significant resonance stabilization and are thus prone to hydrogen abstraction making them relatively poor chain-growth monomers but excellent thiol-ene step-growth monomers. Based on the set of FTIR results, allyl esters were expected to behave similarly. However, unlike vinyl esters, allyl esters have the advantage of being more widely commercially available due to their ease of synthesis and shelf stability. In this regard, it is also foreseeable that the requisite monomers for further photopolymerizable thermoplastic systems that are analogous to other high performance polyesters such as poly(ethylene naphthalate) or poly(butylene succinate) can be arrived at in scale. In general, while relatively less studied than other vinyls (such as allyl ethers, vinyl ethers and norbornenes),[43] both allyl and vinyl esters represent highly promising ene groups that deserve greater attention for broader thiol-ene applications.

It is well established that thermoplastic polymers only develop sufficiently high and useful mechanical properties at critical molecular weight values.[40] To verify the molecular weights measured via SEC-MALS-IV were sufficiently high for practical use, uniaxial tensile tests of 150 μm thick HDT-DAT dogbones (ASTM D638 Type V) were conducted with the key mechanical properties summarized in Table 1. As shown in the engineering stress-strain plot in Figure 2C, characteristic necking followed by significant amounts of strain hardening were observed to occur at elastomeric-like elongations (~800%) suggesting significant amounts of entanglements of the amorphous phase. Interestingly, HDT-DAT exhibited a peculiar plastic deformation mechanism during the strain hardening phase, which consisted of periodic reductions in stress at elevated strains. This behavior was physically observed on the deformed sample as intermittent striations with alternating lines of white, opaque regions and translucent regions (Supporting Information Figure S3). Overall these semicrystalline linear polymers exhibited extremely ductile behavior achieving ultimate tensile strengths of approximately 24 MPa with a toughness of 102 MJ/m^3. While the accessible range of tensile strengths and Young's moduli of these photopolymerizable thermoplastics are lower than the conventional polyesters ($\sigma_{failure}$ ~ 100 MPa), they fail at significantly higher strains thus achieving comparable toughness values. In this respect, photopolymerizable thermoplastics represents a highly unique class of polymeric materials that can be easily tuned to meet a desired set of physical (T_g and T_m) and mechanical properties based on monomer structure(s) and their purity.

Table 1. Summarized mechanical properties of HDT-DAT obtained from the stress-strain behavior due to uniaxial tensile tests performed at a strain rate of 5 mm/min.

Stoichiometric HDT-DAT photopolymerizable thermoplastic	
Young's modulus (MPa)	75 ± 5
Yield strength (MPa)	7 ± 1
Ultimate tensile strength (MPa)	24 ± 2
Failure strain (%)	793 ± 25
Toughness (MJ/m^3)	102 ± 9

Given its exceptional mechanical properties, the HDT-DAT system was used to assess the viability of photopolymerizable thermoplastics towards SLA 3D printing. Initial 2D photopatterning experiments were conducted using a

commercial digital light processing (DLP) system as well as a scanning laser microscope to record arbitrary patterns on the same HDT-DAT system. Given the additional consideration of crystallization, caveats of photopatterning photopolymerizable thermoplastics exist. With DLP patterning, a well resolved Ralphie™ (the buffalo mascot of the University of Colorado at Boulder) was successfully patterned (Figure 3A). In the case of patterning with a high intensity scanning laser, noticeable over-cure was observed as seen in the differential interference contrast image in Figure S4 whereby spherulites formed within tens of seconds of irradiation outside the intended red shaded square irradiation pattern. This result is explained by the combination of rapid polymerization within a low viscosity medium without any significant inhibiting species to confine reaction-diffusion. These results suggest that spatial resolution control (i.e. control over the crystallization) in photopolymerizable thermoplastics is highly dependent on exposure intensity and viscosity. To address the issue of over-curing, carbon black was used as a photoabsorber in an otherwise unoptimized SLA 3D printing formulation. Printing of photopolymerizable thermoplastics was validated using two different commercial SLA 3D printers. First, as shown in Figure 3B, using a production-grade LED-based 3D printer, excellent spatial resolutions (pillar diameters as low as 400 μm) were obtained from a standard quality control (QC) test print in addition to other simple objects. Next, using a more affordable desktop projector-based 3D printer, detailed prints were also demonstrated with the standard Marvin test print in addition to the printing of other solid parts with substantial bulky overhanging features as shown in Figure 3C. Nevertheless, the lack of oxygen inhibition coupled with the interplay of rapid reactivity and crystallization does make resin-based 3D printing of such thiol-ene resins less straightforward compared to conventional (meth)acrylate systems such as the additional consideration of shrinkage due to crystallization to supplement the polymerization-induced shrinkage. While shrinkage for either process was not measured here, one or both could be issues for additive manufacturing for some photopolymerizable thermoplastic systems.

The high levels of intricacy and customization afforded by 3D printing offer tremendous potential for a variety of applications for meltable additive manufacturing resins. Specifically, with respect to jewelry investment or other casting, current 3D printing approaches involve printing the positive of a ring, or set of rings, that eventually serve as a sacrifice after casting in gypsum. Since all existing resins form crosslinked polymers, the embedded prints within the set gypsum need to be burnt off at polymer decomposition temperatures often in excess of 500°C for removal. This process is tedious and ultimately imperfect as residual ash and residue limit final resolutions and the desired object's quality and finish, especially for jewelry and other high-value products. This same concept of decomposing a sacrificial printed photopolymer is also employed for 3D printing ceramics.[44] In these instances, the ability to simply melt an embedded print and flow out the polymer represents an enabling advancement over current methods. We demonstrate this capability with photopolymerizable thermoplastics in Figure 3D by placing a glass slide with upright printed pillar structures on a hotplate set at 90°C. Within a minute, the base of the print in contact with the slide melted into a liquid causing the individual pillars to wilt and topple down before eventually melting as well, as shown in the supplementary video. The resulting melt was then shown to be easily manipulated with the tip of a glass pipette to draw an abstract design.

COMMUNICATION

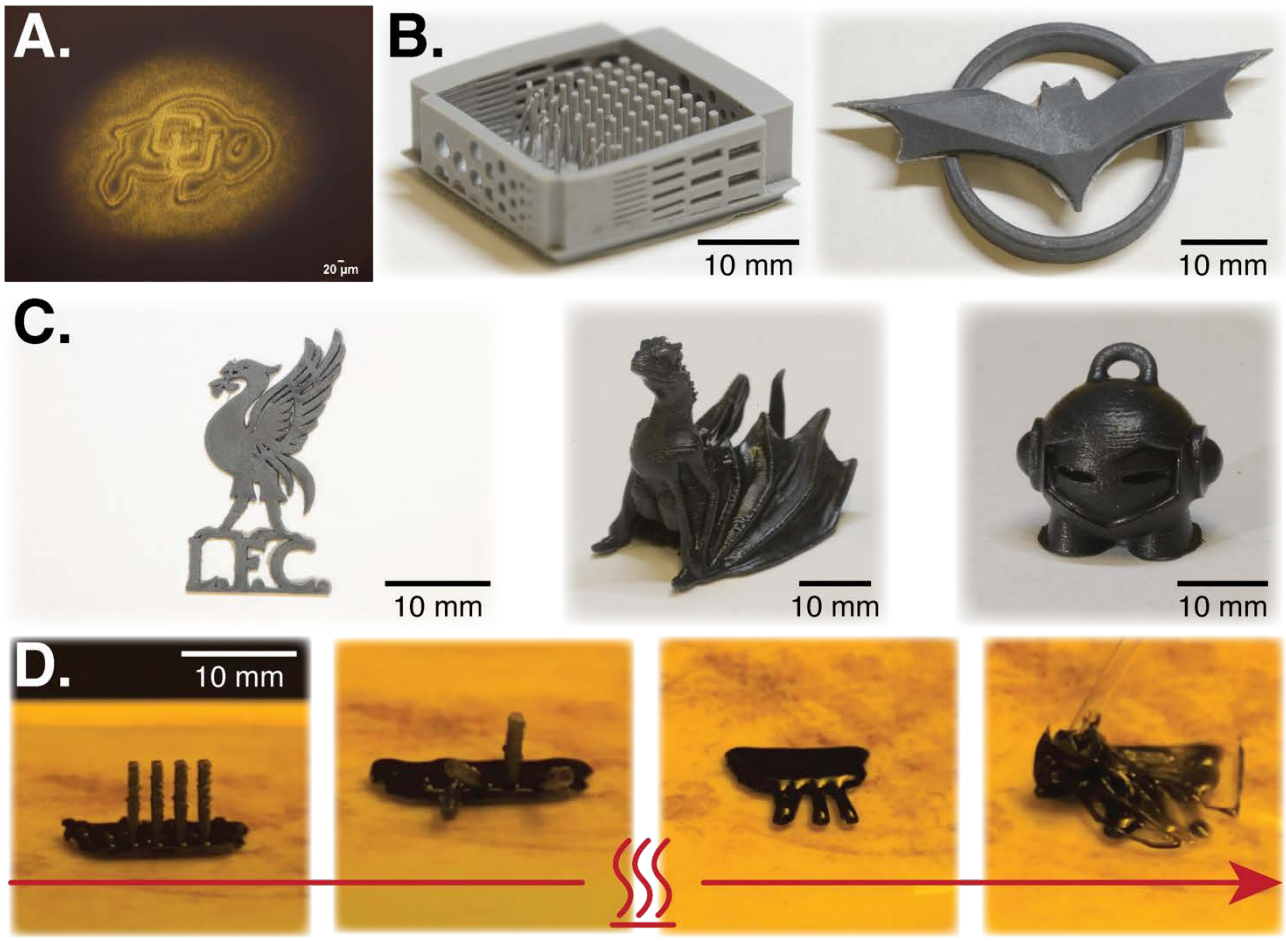

Figure 3. Photopatterning via digital light processing (DLP), 3D printed objects and melting of 3D printed HDT-DAT photopolymerizable thermoplastics. a) A brightfield image of a buffalo is patterned on neat HDT-DAT resin using a 400 nm LED and a DLP. b) Photographs of 3D printed objects (QC, batarang and a ring) printed using a production-grade LED-based 3D printer. c) Photographs of SLA 3D printed objects using an desktop projector-based 3D printer. (d) 3D printed pillars on a glass slide that was placed on a hotplate set at 90°C. As a result, rapid melting and liquification was observed with the base of the part first to soften and melt, causing the initially upright pillars to wilt, fall and follow suit in melting.

While essentially all thermoplastics are inherently recyclable, the unfortunate reality is that less than 10% of all plastics get recycled[45] with PET being the most recycled polymer. A contributing reason for this is the relative economics, i.e. extremely low costs of production for low value end uses in contrast to the steep costs of sorting and recycling. Unlike conventional thermoplastics, photopolymerizable thermoplastics are likely to only be economically feasible for high value applications such as additive manufacturing. Hence, they are less likely to be used for short single-use (typically low value) applications and more likely to be recycled and sustainable, possibly alleviating the issue of 3D printing exacerbating the plastics waste problem with permanent crosslinked polymers. In fact, a valuable feature of photopolymerizable thermoplastics is its intrinsic reprocessability. This lends to the concept of being able to reuse a SLA printed object (or cured resin) as a feedstock for one of the alternative 3D printing methods such as fused deposition modeling (FDM) and material jetting. As these additive manufacturing techniques fundamentally rely on the deposition of melted materials, printed photopolymerizable thermoplastics at the end of their SLA lifetime can be recycled for use as 'new' resins for FDM. Used in this manner, the crystalline structure and properties of the polymer could be recovered or possibly even enhanced due to the thermal processing.

The practical factors that may limit viability of the thiol-ene chemistry as 3D printing resins are primarily shelf-life resin stability and the unpleasant odor. In the former case, it has been

well established that thiol-ene resin stability can vary widely from a few hours to multiple months with multiple strategies reported to effectively address this.[46] Within the scope of the studied photopolymerizable thermoplastic thiol-ene systems and with minimal attempts to stabilize the system, a stability of a few days was observed with 1,2-ethane dithiol-based (EDT) systems. Given the low starting viscosities of these thiol-ene thermoplastic systems, the finite stability of the resin can actually be considered useful in the slow and gradual generation of low molecular weight oligomers for reducing odor (primarily due to low molecular weight thiols) without dramatically compromising print quality. Furthermore, as mentioned earlier, any reacted photopolymerizable thermoplastics resin can simply be repurposed instead of discarded. Finally, while the issue of odor is more of an inconvenience issue than of toxicity (unlike with many acrylates), several measures can be taken to mitigate the overall smell. A simple chemical approach would be to pre-oligomerize the resin to form higher molecular weight species while more direct strategies such as printing in a fume hood or having a vapor extraction system could also be considered.

Conclusions

To summarize, the first instance of mechanically robust linear polymeric materials made via photopolymerization and applied towards SLA 3D printing is disclosed. Enabled by the rapid and quantitative thiol-ene 'click' reaction, semicrystalline linear high molecular weight polymers are readily obtained in seconds using low intensity light. These photopolymerizable thermoplastics represent a unique sub-class of polymeric materials possessing an exceptional combination of tensile strength, elongation and toughness. A thorough validation of thermoplastic printability was demonstrated using commercial DLP-based 3D printers for a set of variable objects and parts including the well-recognized Marvin printing standard. Critically, the intrinsic ability to melt and reprocess these otherwise tough materials lends itself to a variety of uses not achievable with current photopolymers. It is envisioned that further research on photopolymerizable thermoplastics will greatly expand upon the range of material properties accessible with light, thus enabling a multitude of unrealized 3D printing applications.

Conflicts of interest

A provisional patent on this work has been filed by the Venture Partners at University of Colorado Boulder.

Notes and references

‡ Footnotes relating to the main text should appear here. These might include comments relevant to but not central to the matter under discussion, limited experimental and spectral data, and crystallographic data.
§
§§

etc.

1. I. Gibson, *Additive Manufacturing Technologies*, Springer, New York, 2014.
2. T. D. Ngo, A. Kashani, G. Imbalzano, K. T. Q. Nguyen and D. Hui, *Composites Part B: Engineering*, 2018, **143**, 172-196.
3. S. C. Ligon, R. Liska, J. Stampfl, M. Gurr and R. Mulhaupt, *Chem. Rev.*, 2017, **117**, 10212-10290.
4. M. Layani, X. F. Wang and S. Magdassi, *Adv. Mater.*, 2018, **30**, 7.
5. J. W. Stansbury and M. J. Idacavage, *Dent. Mater.*, 2016, **32**, 54-64.
6. X. Chen, W. Liu, B. Dong, J. Lee, H. O. T. Ware, H. F. Zhang and C. Sun, *Adv. Mater.*, 2018, **30**, 1705683.
7. M. P. de Beer, H. L. van der Laan, M. A. Cole, R. J. Whelan, M. A. Burns and T. F. Scott, *Sci. Adv.*, 2019, **5**, eaau8723.
8. J. R. Tumbleston, D. Shirvanyants, N. Ermoshkin, R. Janusziewicz, A. R. Johnson, D. Kelly, K. Chen, R. Pinschmidt, J. P. Rolland, A. Ermoshkin, E. T. Samulski and J. M. DeSimone, 2015, **347**, 1349-1352.
9. M. Shusteff, A. E. M. Browar, B. E. Kelly, J. Henriksson, T. H. Weisgraber, R. M. Panas, N. X. Fang and C. M. Spadaccini, *Sci. Adv.*, 2017, **3**, eaao5496.
10. B. E. Kelly, I. Bhattacharya, H. Heidari, M. Shusteff, C. M. Spadaccini and H. K. Taylor, *Science*, 2019, DOI: 10.1126/science.aau7114, eaau7114.
11. B. Zhang, K. Kowsari, A. Serjouei, M. L. Dunn and Q. Ge, *Nat. Commun.*, 2018, **9**, 1831.
12. J. J. Schwartz and A. J. Boydston, *Nat. Commun.*, 2019, **10**, 791.
13. N. D. Dolinski, Z. A. Page, E. B. Callaway, F. Eisenreich, R. V. Garcia, R. Chavez, D. P. Bothman, S. Hecht, F. W. Zok and C. J. Hawker, *Adv. Mater.*, 2018, **30**, 1800364.
14. J. Poelma and J. Rolland, *Science*, 2017, **358**, 1384-1385.
15. D. K. Patel, A. H. Sakhaei, M. Layani, B. Zhang, Q. Ge and S. Magdassi, *Adv. Mater.*, 2017, **29**, 1606000.
16. M. Hegde, V. Meenakshisundaram, N. Chartrain, S. Sekhar, D. Tafti, C. B. Williams and T. E. Long, *Adv. Mater.*, 2017, **29**, 1701240.
17. J. Herzberger, V. Meenakshisundaram, C. B. Williams and T. E. Long, *ACS Macro Lett.*, 2018, **7**, 493-497.
18. K. Seidler, M. Griesser, M. Kury, R. Harikrishna, P. Dorfinger, T. Koch, A. Svirkova, M. Marchetti-Deschmann, J. Stampfl, N. Moszner, C. Gorsche and R. Liska, *Angew Chem Int Ed Engl*, 2018, **57**, 9165-9169.
19. Q. Shi, K. Yu, X. Kuang, X. Mu, C. K. Dunn, M. L. Dunn, T. Wang and H. J. Qi, *Mater. Horizons*, 2017, **4**, 598-607.
20. D. G. Sycks, T. Wu, H. S. Park and K. Gall, *Journal of Applied Polymer Science*, 2018, **135**, 46259.
21. N. Bhattacharjee, C. Parra-Cabrera, Y. T. Kim, A. P. Kuo and A. Folch, *Adv. Mater.*, 2018, **30**, 1800001.
22. C. J. Thrasher, J. J. Schwartz and A. J. Boydston, *ACS Appl. Mater. Interfaces*, 2017, **9**, 39708-39716.
23. H. Leonards, S. Engelhardt, A. Hoffmann, L. Pongratz, S. Schriever, J. Bläsius, M. M. Wehner and A. Gillner, *Proceedings of SPIE*, 2015, **9353**, 7.
24. L. Chen, Q. Wu, G. Wei, R. Liu and Z. Li, *Journal of Materials Chemistry C*, 2018, **6**, 11561-11568.
25. T. J. Wallin, J. H. Pikul, S. Bodkhe, B. N. Peele, B. C. Mac Murray, D. Therriault, B. W. McEnerney, R. P. Dillon, E. P.

Giannelis and R. F. Shepherd, *Journal of Materials Chemistry B*, 2017, **5**, 6249-6255.
26. A. Bagheri and J. Jin, *ACS Applied Polymer Materials*, 2019, **1**, 593-611.
27. H. B. Song, A. Baranek, B. T. Worrell, W. D. Cook and C. N. Bowman, *Adv. Funct. Mater.*, 2018, **28**, 9.
28. K. Jin, E. K. Leitsch, X. Chen, W. H. Heath and J. M. Torkelson, *Macromolecules*, 2018, **51**, 3620-3631.
29. D. Zhang and M.-J. Dumont, *Polymer Chemistry*, 2018, **9**, 743-756.
30. H. Li, S. Thanneeru, L. Jin, C. J. Guild and J. He, *Polymer Chemistry*, 2016, **7**, 4824-4832.
31. O. van den Berg, T. Dispinar, B. Hommez and F. E. Du Prez, *Eur. Polym. J.*, 2013, **49**, 804-812.
32. W. H. Carothers, *Chem. Rev.*, 1931, **8**, 353-426.
33. F. Jasinski, E. Lobry, B. Tarablsi, A. Chemtob, C. Croutxé-Barghorn, D. Le Nouen and A. Criqui, *ACS Macro Lett.*, 2014, **3**, 958-962.
34. F. Jasinski, A. Rannée, J. Schweitzer, D. Fischer, E. Lobry, C. Croutxé-Barghorn, M. Schmutz, D. Le Nouen, A. Criqui and A. Chemtob, *Macromolecules*, 2016, **49**, 1143-1153.
35. H. Mark, *Industrial & Engineering Chemistry*, 1942, **34**, 1343-1348.
36. G. Reiter and G. R. Strobl, *Progress in understanding of polymer crystallization*, Springer, 2007.
37. L. Mandelkern, *Crystallization of polymers*, Cambridge Univ Press, [Place of publication not identified], 2010.
38. A. G. Shtukenberg, Y. O. Punin, E. Gunn and B. Kahr, *Chem. Rev.*, 2012, **112**, 1805-1838.
39. B. Crist and J. M. Schultz, *Prog. Polym. Sci.*, 2016, **56**, 1-63.
40. G. G. Odian, 2004.
41. A. Mautner, X. Qin, H. Wutzel, S. C. Ligon, B. Kapeller, D. Moser, G. Russmueller, J. Stampfl and R. Liska, *J. Polym. Sci. Part A: Polym. Chem.*, 2013, **51**, 203-212.
42. T. Alfrey and C. C. Price, *J. Polym. Sci.*, 1947, **2**, 101-106.
43. B. H. Northrop and R. N. Coffey, *J. Am. Chem. Soc.*, 2012, **134**, 13804-13817.
44. J. W. Halloran, *Annual Review of Materials Research*, 2016, **46**, 19-40.
45. J. M. Garcia and M. L. Robertson, 2017, **358**, 870-872.
46. P. Esfandiari, S. C. Ligon, J. J. Lagref, R. Frantz, Z. Cherkaoui and R. Liska, 2013, **51**, 4261-4266.

Conceptual Insights

Thermoplastics, such as poly(ethylene) and poly(ethylene terephthalate), are high molecular weight linear polymers that have become the preeminent synthetic materials of modern society for applications as diverse as structural materials and drug delivery. Photopolymers, in contrast, are usually crosslinked materials conveniently fabricated from low viscosity liquid resins in a matter of seconds upon exposure to light. Thermoplastics formed from photopolymerizations, however, either do not develop sufficiently useful material properties compared to traditional manufacturing methods such as injection molding or extrusion, or, do not develop those properties in reasonable timescales necessitated by photopolymerization-based curing. Here, a new instance of photopolymerizable thermoplastics is reported whereby semicrystalline high molecular weight noncrosslinked polymers are formed with less than 5 seconds of visible light exposure at ambient conditions using low intensities (1-10 mW/cm^2). This distinct approach enables access to an extraordinary set of mechanical properties and capabilities not achievable with current photopolymers such as a tough material with ultimate tensile strengths of 24 MPa at failure elongations of 800% that is subsequently meltable and reprocessable at elevated temperatures. Harnessing these photopolymerizable thermoplastics for vat photopolymerization-based 3D printing, a collection of high resolution parts were readily printed using commercial printers including the classical Marvin test print.